J|A|C|S
ARTICLES
Published on Web 11/04/2006

Lipid Lateral Mobility and Membrane Phase Structure Modulation by Protein Binding

Martin B. Forstner,[†] Chanel K. Yee,[‡] Atul N. Parikh,[‡] and Jay T. Groves*[,†,§]

Contribution from the Department of Chemistry, University of California, Berkeley, California 94720, Department of Applied Science, University of California, Davis, California 95616, and Physical Biosciences and Material Sciences Division, Lawrence Berkeley National Laboratory, Berkeley, California 94720

Received June 9, 2006; E-mail: JTGroves@lbl.gov

Abstract: Using a combination of fluorescence correlation and infrared absorption spectroscopies, we characterize lipid lateral diffusion and membrane phase structure as a function of protein binding to the membrane surface. In a supported membrane configuration, cholera toxin binding to the pentasaccharaide headgroup of membrane-incorporated GM_1 lipid alters the long-range lateral diffusion of fluorescently labeled probe lipids, which are not involved in the binding interaction. This effect is prominently amplified near the gel-fluid transition temperature, T_m, of the majority lipid component. At temperatures near T_m, large changes in probe lipid diffusion are measured at average protein coverage densities as low as 0.02 area fraction. Spectral shifts of the methylene symmetric and asymmetric stretching modes in the lipid acyl chain confirm that protein binding alters the fraction of lipid in the gel phase.

1. Introduction

The fluidity of cell membranes is critical to their biological functions. Assembly of membrane proteins into signaling complexes and large scale reorganization of the cell surface are all influenced by lateral mobility of membrane lipids.[1−4] The underlying lipid bilayer structure of cell membranes exhibits a rich phase behavior, which can significantly influence molecular movement within the membrane.[5−8] The phase structure of cell membranes has attracted much attention, and diffusion measurements have been widely used as probes to characterize both simple lipid bilayers and live cell membranes.[9−14]

Trajectories of unencumbered molecular Brownian motion exhibit a characteristic linear scaling of the mean square displacement ($\langle r^2 \rangle$) with time (t). This provides a convenient definition of the diffusion coefficient (D) as the constant of proportionality: $\langle r^2 \rangle = 4Dt$, in two dimensions.[15,16] The diffusion coefficient represents an integrated measure of molecular mobility through the surrounding environment. As such, it is intrinsically circumstantial. The diffusion of one species in a mixture is reflective of the overall composition, as well as any heterogeneities within the system. Measurements of diffusion inherently depend on the length scales probed by the particular choice of technique. Electron spin resonance (ESR)[17,18] and conventional nuclear magnetic resonance (NMR)[19] are useful for probing lipid motions in membranes on the nanometer scale of next neighbor interactions. Stimulated spin−echo NMR may probe up to 100 nm.[20,21] For length scales larger than a micron, fluorescence recovery after photobleaching (FRAP)[22−24] along with single particle[25,26] and fluorophore tracking[27] have been widely applied in membrane systems. In cell membranes, molecular movements on the 100−1000 nm length scale are

[†] University of California, Berkeley.
[‡] University of California, Davis.
[§] Lawrence Berkeley National Laboratory.

(1) Engelman, D. M. *Nature* **2005**, *438*, 578−580.
(2) Edidin, M. *Nat. Rev. Mol. Cell. Biol.* **2003**, *4*, 414−418.
(3) Vereb, G.; Szollosi, J.; Matko, J.; Nagy, P.; Farkas, T.; Vigh, L.; Matyus, L.; Waldmann, T. A.; Damjanovich, S. *Proc. Natl. Acad. Sci. U.S.A.* **2003**, *100*, 8053−8058.
(4) Anderson, R. G. W.; Jacobson, K. *Science* **2002**, *296*, 1821−1825.
(5) Bacia, K.; Schwille, P.; Kurzchalia, T. *Proc. Natl. Acad. Sci. U.S.A.* **2005**, *102*, 3272−3277.
(6) Hammond, A. T.; Heberle, F. A.; Baumgart, T.; Holowka, D.; Baird, B.; Feigenson, G. W. *Proc. Natl. Acad. Sci. U.S.A.* **2005**, *102*, 6320−6325.
(7) Baumgart, T.; Hess, S. T.; Webb, W. W. *Nature* **2003**, *425*, 821−824.
(8) Simons, K.; Ikonen, E. *Nature* **1997**, *387*, 569−572.
(9) Kusumi, A.; Nakada, C.; Ritchie, K.; Murase, K.; Suzuki, K.; Murakoshi, H.; Kasai, R. S.; Kondo, J.; Fujiwara, T. *Annu. Rev. Biophys. Biomol. Struct.* **2005**, *34*, 351−U354.
(10) Lippincott-Schwartz, J.; Snapp, E.; Kenworthy, A. *Nat. Rev. Mol. Cell. Biol.* **2001**, *2*, 444−456.
(11) Dietrich, C.; Bagatolli, L. A.; Volovyk, Z. N.; Thompson, N. L.; Levi, M.; Jacobson, K.; Gratton, E. *Biophys. J.* **2001**, *80*, 1417−1428.
(12) Winckler, B.; Forscher, P.; Mellman, I. *Nature* **1999**, *397*, 698−701.
(13) Korlach, J.; Schwille, P.; Webb, W. W.; Feigenson, G. W. *Proc. Natl. Acad. Sci. U.S.A.* **1999**, *96*, 8461−8466.
(14) Jacobson, K.; Sheets, E. D.; Simson, R. *Science* **1995**, *268*, 1441−1442.
(15) Einstein, A. *Analen der Physik* **1905**, *15*, 549.
(16) Chandrasekhar, S. *Rev. Mod. Phys.* **1943**, *15*, 1−89.
(17) Hubbell, W. L.; McConnel, H. M. *Proc. Natl. Acad. Sci. U.S.A.* **1969**, *64*, 20−27.
(18) Hubbell, W. L.; McConnel, H. M. *Proc. Natl. Acad. Sci. U.S.A.* **1969**, *63*, 16−22.
(19) Stejskal, E. O.; Tanner, J. E. *J. Chem. Phys.* **1965**, *42*, 288−292.
(20) Kuo, A. L.; Wade, C. G. *Chem. Phys. Lipids* **1979**, *25*, 135−139.
(21) Tanner, J. E. *J. Chem. Phys.* **1970**, *52*, 2523−2526.
(22) Jacobson, K.; Elson, E.; Koppel, D.; Webb, W. *Nature* **1982**, *295*, 283−284.
(23) Schlessinger, J.; Axelrod, D.; Koppel, D. E.; Webb, W. W.; Elson, E. L. *Science* **1977**, *195*, 307−309.
(24) Axelrod, D.; Koppel, D. E.; Schlessinger, J.; Elson, E.; Webb, W. W. *Biophys. J.* **1976**, *16*, 1055−1069.
(25) Lee, G. M.; Ishihara, A.; Jacobson, K. A. *Proc. Natl. Acad. Sci. U.S.A.* **1991**, *88*, 6274−6278.
(26) Saxton, M. J.; Jacobson, K. *Annu. Rev. Biophys. Biomol. Struct.* **1997**, *26*, 373−399.
(27) Schmidt, T.; Schutz, G. J.; Baumgartner, W.; Gruber, H. J.; Schindler, H. *Proc. Natl. Acad. Sci. U.S.A.* **1996**, *93*, 2926−2929.

particularly important, and this scale is conveniently probed by fluorescence cross correlation spectroscopy (FCS).[28−32]

Here, we combine structural information from attenuated total reflection Fourier transform infrared spectroscopy (ATR-FTIRS) and mesoscopic diffusion measurements, obtained with FCS, to characterize the effects of protein binding on the membrane surface. Experiments were performed in the supported bilayer configuration, which is widely utilized as a model membrane system for biophysical studies. Lipid diffusion has been studied in relation to the binding of proteins[33,34] and adsorption of polymers[35] on the supported membrane surface. The present investigation is stimulated by unusually large changes in lipid mobility that have been observed at low protein coverage densities (0.02 area fraction) near the gel-fluid transition temperature, T_m, of DMPC supported membranes.[33] We specifically seek to resolve the ternary relationship among protein binding, membrane phase, and long-range lipid mobility.

Above the membrane melting temperature, T_m, the L_β gel phase gives way to the fluid L_α phase. This transition involves a highly cooperative melting of the all-trans configuration of the lipid acyl chains in the gel phase. Above T_m, the methylene groups can rotate about the C−C bonds, allowing the chains to assume gauche configurations as well. While acyl chains are orientationally ordered over many lipids in the gel phase, no long-range correlation in chain alignment exists in the fluid phase.[36−38] Since chain conformation and the degree of long-range order are intimately related,[39,40] both can be inferred from infrared spectra of the vibrational stretching modes of the acyl chains methylenes. The structural difference between the two phases is also mirrored in their respective diffusion properties, with slow diffusion in the gel phase and faster diffusive transport in the fluid phase.[41] A similar relation is likewise found in cholesterol containing lipid mixtures that exhibit miscibility phase separation into liquid ordered (l_o) and liquid disordered phases (l_d). Lacking long-range orientational chain order, both of these phases are liquidlike.[13,42] While interrelations between structure and dynamic properties have been well studied on the molecular scale in pure phases, many questions remain concerning long range transport in membranes exhibiting phase coexistence. This is especially pertinent as molecular mobility observations are increasingly used as probes of membrane structure and organization.[9,14,43]

In the results described below, binding of cholera toxin subunit B (CTB) to its membrane surface ligand, ganglioside GM_1, is found to nucleate appreciable conformational lipid ordering at temperatures as far as 15 °C above T_m. Diffusion of probes, which are not involved in the binding, however, exhibits a different response. Away from the transition, only a marginal change in mobility is observed between the bound and unbound scenarios; protein binding has little influence on lipid mobility in fully fluid membranes. In this case, the effective long-range diffusion is well described by a model based on protein induced impermeable diffusion obstacles. In contrast, near the transition, a significant reduction in lipid mobility results from protein binding down to coverage densities as low as 0.02 area fraction.

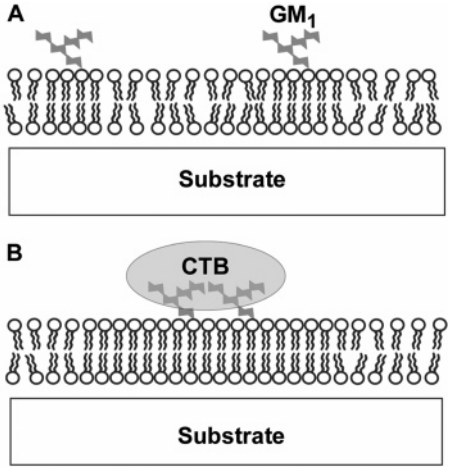

Figure 1. Schematic of increased order due to CTB binding to GM_1 close to the lipid melting transition. (A) Without the ordering effect of membrane bound protein, the fluid phase can develop freely. (B) CTB binding retards the formation of the fluid phase by extending the ordered gel phase beyond the CTB−GM_1 binding site.

These structural and dynamical observations can be reconciled by a cooperative mechanism in which protein binding nucleates nanometer scale gel phase domains that propagate beyond the immediate binding site, as illustrated schematically in Figure 1. In order for these localized regions of gel phase to strongly influence long-range lipid mobility, they must modify the gel-fluid coexistence regime. Comparison of FCS and ATR-FTIRS results presented below support this model and provide evidence for nonlocal effects of protein binding on membrane phase structure. These observations underscore the extremely responsive nature of lipid membranes near phase transitions and illustrate the ease with which proteins may modulate such structures.

2. Materials and Methods

Detailed descriptions of the materials, the methods, the techniques, and the data analysis of the experiments are contained in the Supporting Information. In brief, for the attenuated total reflection Fourier transform infrared (ATR-FTIR) spectroscopy, single bilayer DMPC membranes doped with 0.5 mol % GM_1 ganglioside were formed on a silicon internal reflection element (IRE), (Figure 6A). Infrared absorption spectra where taken in the presence and the absence of GM_1 binding Cholera toxin subunit B (CTB) protein as a function of temperature in the range from 19 to 45 °C (Figure 6B and 6C).

The basic experimental configuration of the fluorescence correlation spectroscopy (FCS) set up is schematically depicted in Figure 2A.

To enable FCS experiments, membranes containing the main lipid (DMPC or DMOPC), 0.5 mol % GM_1 and also 0.005 mol % of a Bodipy FL labeled lipid analogue were supported on glass cover slides (Figure 2A, inset). Resulting average correlations in the presence and

(28) Sanchez, S. A.; Gratton, E. *Acc. Chem. Res.* **2005**, *38*, 469−477.
(29) Bacia, K.; Scherfeld, D.; Kahya, N.; Schwille, P. *Biophys. J.* **2004**, *87*, 1034−1043.
(30) Haustein, E.; Schwille, P. *Methods* **2003**, *29*, 153−166.
(31) Hess, S. T.; Huang, S. H.; Heikal, A. A.; Webb, W. W. *Biochemistry* **2002**, *41*, 697−705.
(32) Fahey, P. F.; Koppel, D. E.; Barak, L. S.; Wolf, D. E.; Elson, E. L.; Webb, W. W. *Science* **1977**, *195*, 305−306.
(33) Yamazaki, V.; Sirenko, O.; Schafer, R. J.; Groves, J. T. *J. Am. Chem. Soc.* **2005**, *127*, 2826−2827.
(34) Wagner, M. L.; Tamm, L. K. *Biophys. J.* **2001**, *81*, 266−275.
(35) Zhang, L. F.; Granick, S. *Proc. Natl. Acad. Sci. U.S.A.* **2005**, *102*, 9118−9121.
(36) Marsh, D. *Chem. Phys. Lipids* **1991**, *57*, 109−120.
(37) Laggner, P.; Kriechbaum, M. *Chem. Phys. Lipids* **1991**, *57*, 121−145.
(38) Cevc, G. *Chem. Phys. Lipids* **1991**, *57*, 293−307.
(39) Casal, H. L.; Mantsch, H. H. *Biochim. Biophys. Acta* **1984**, *779*, 381−401.
(40) Lewis, R.; McElhaney, R. N. *Chem. Phys. Lipids* **1998**, *96*, 9−21.
(41) Tocanne, J. F.; Dupoucezanne, L.; Lopez, A. *Prog. Lipid Res.* **1994**, *33*, 203−237.
(42) Vist, M. R.; Davis, J. H. *Biochemistry* **1990**, *29*, 451−464.
(43) Ratto, T. V.; Longo, M. L. *Biophys. J.* **2002**, *83*, 3380−3392.

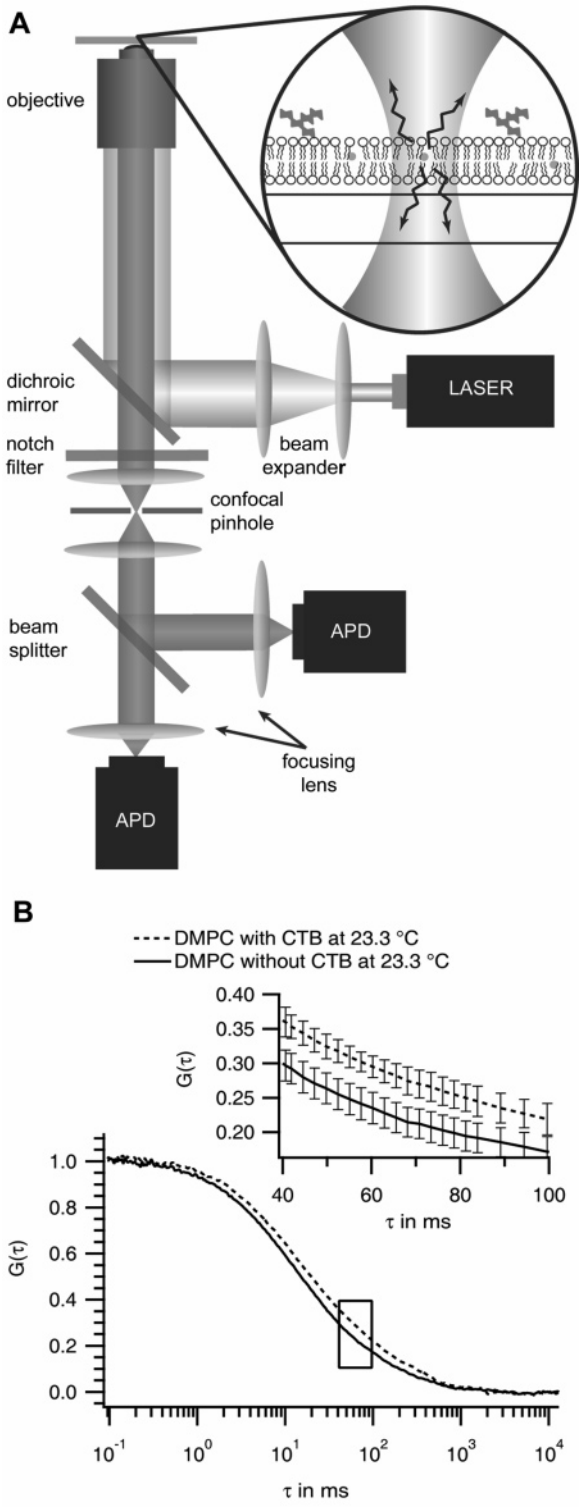

Figure 2. (A) Schematic of the FCS apparatus (for detailed description see main text). Fluorescently labled lipids diffusing through the focused laser spot, emitting photons while crossing the excitation area (A, inset). (B) Cross-correlation curves from membranes with (solid line) and without bound CTB (dotted line) close to the melting transition. Their difference can be resolved, given the accuracy of the measurement indicated by the error bars in the magnification of the boxed region (inset).

absence of CTB are shown as examples in Figure 2B. They represent FCS measurements on the fluorescent lipid probes in DMPC membranes doped with GM_1 at a temperature of 23.3 ± 0.3 °C. At that temperature the membranes are close to the main transition of DMPC (T_m = 23° C).[48] The solid line corresponds to measurements on SLB without CTB, while the correlation curve, after CTB has bound to GM_1, is drawn with a dashed line. In the magnification of the boxed region of the curves (Figure 2B inset), where the standard deviations are represented as error bars on each point, the separation of the two curves including their error bands is distinct. Hence, it is assured that the changes in mobility for different conditions can be resolved given the accuracy of our FCS measurements. The diffusion coefficients of the fluorescent lipid probe were obtained by fitting the experimental correlation curves to the appropriate analytical expression as described in the Supporting Information.

3. Results and Discussion

3.1. Temperature-Dependent Diffusion Measurements. Below we present measurements of the effect of protein binding on the mobility of lipids in the membrane as a function of temperature in the range from 19 to 45 °C. Diffusion coefficients of the Bodipy-FL HPC lipids in GM_1-doped DMPC and DMOPC membranes were measured using FCS in the presence and absence of CTB or anti-GM_1 antibody. DMPC membranes exhibit a gel to the fluid phase transition within the investigated temperature range, while DMOPC membranes remain exclusively in the fluid L_α phase and served as control.

In the absence of GM_1 binding proteins, the measured diffusion coefficients for the fluorescent Bodipy-FL HPC lipid probe (Figure 3A, circles) show good agreement with previously published values.[41] As expected, lipids diffuse slowly in the gel phase (0.9 ± 0.1 $\mu m^2/s$), experience a sudden increase in mobility with the onset of the main transition at T_m = 23 °C, and steadily gain higher diffusivity upon further heating. When CTB is bound to GM_1 moieties (Figure 3A, squares), the onset of rapid diffusion occurs at 25 °C, 2 °C above T_m. Beyond the transition region, lipid diffusion in the CTB-bound membranes remains slightly lower than that in protein-free DMPC membranes. A qualitatively similar behavior was observed when anti-GM_1 antibody (~500 nM) was allowed to bind to the GM_1-containing DMPC membrane (Figure 3A, diamonds). However, antibody binding results in a less pronounced retardation of lipid mobility. This most likely results from less stringent constraints imposed by bound antibodies on the arrangement of the proximal lipids at the binding site. The y-shaped IgG allows for variable spacing of its two binding sites and covers a smaller area upon binding, whereas the rigid disc-shaped CTB protein possesses five binding sites at fixed locations. The latter would suggest that CTB will be able to impose more order on the membrane underneath, since the bound GM_1 will be held at fixed relative distances. In contrast, in the case of the antibody the lipids underneath should be able to rearrange with much more ease, since a range of distances between the two bound GM_1 can be accommodate by the antibody.

To confirm that the reduction in diffusivity near T_m due to protein binding is indeed connected to the proximity to the main transition, we performed parallel experiments with DMOPC as the majority lipid for comparison. DMOPC differs from DMPC only by a double bond at the C_9 position of each acyl chain,

(44) Mayer, L. D.; Hope, M. J.; Cullis, P. R. *Biochim. Biophys. Acta* **1986**, *858*, 161−168.
(45) Groves, J. T.; Ulman, N.; Boxer, S. G. *Science* **1997**, *275*, 651−653.
(46) Hull, M. C.; Cambrea, L. R.; Hovis, J. S. *Anal. Chem.* **2005**, *77*, 6096−6099.
(47) Brian, A. A.; McConnell, H. M. *Proc. Natl. Acad. Sci. U.S.A.* **1984**, *81*, 6159−6163.
(48) Marsh, D. *Handbook of Lipid Bilayers*; CRC Press: Boca Raton, FL, 1990.

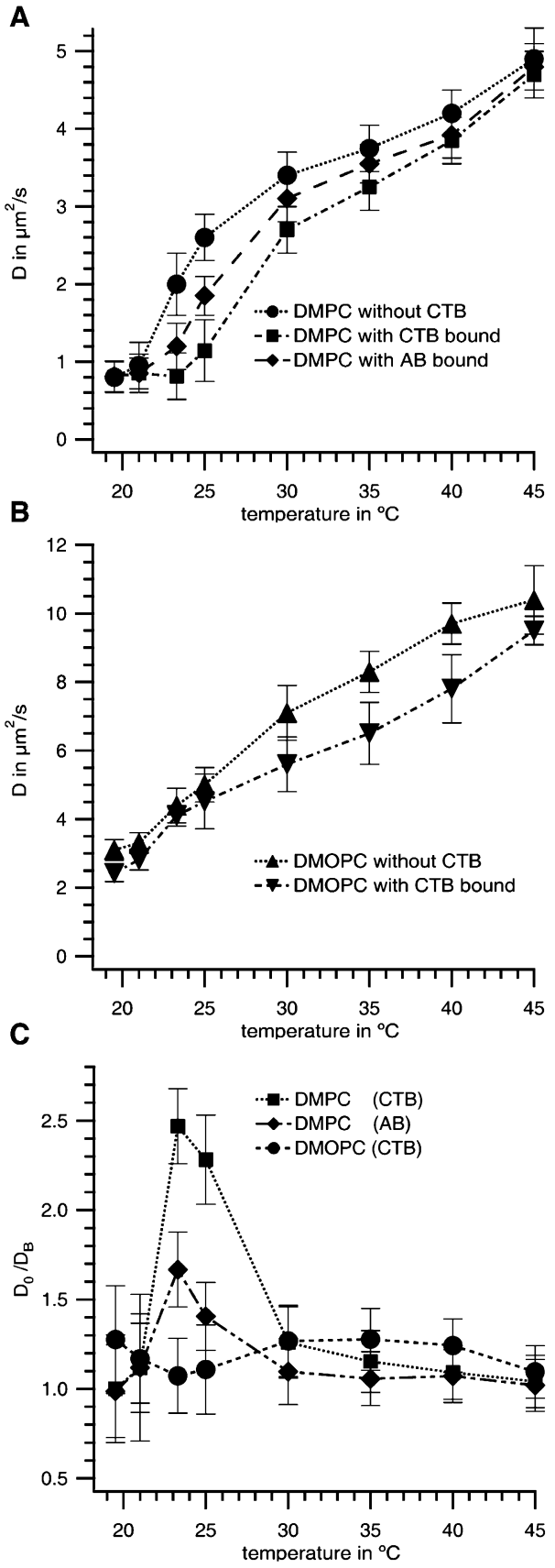

Figure 3. (A) Diffusion coefficients D in DMPC membranes as function of temperature with CTB bound (■), with anti-GM1 antibody bound (◆) and without ligand (●). (B) D for membranes of DMOPC with (▼) and without CTB bound (▲) as function of temperature. (C) The ratio of D_0 (no protein bound) to D_b (protein bound) exhibits different dependence on temperature for DMPC (● (CTB), ◆ (antibody)) and DMOPC (■).

resulting in a gel-fluid T_m for DMOPC of approximately −65 °C.[52] Thus, over the experimental temperature range (19−45 °C), DMOPC membranes are always in the fully conformationally disordered fluid L_α phase. FCS measurements reveal that lipid diffusion accelerates steadily with increasing temperature in DMOPC membranes regardless of whether CTB is bound or not (Figure 3B). While lipid diffusion is slowed by CTB-binding to DMOPC membranes, temperature-dependent discontinuities were not observed.

Differences in the diffusive behavior in DMPC and DMOPC membranes under different protein binding scenarios can be observed most clearly in the ratio of the diffusion coefficient with protein bound, D_b, to D_0 (no protein) (Figure 3C). A disproportional decay in lipid diffusion occurs upon protein binding near the phase transition temperature.

Protein binding to the membrane surface creates obstacles to long-range motion, and the diffusion data can be analyzed using the effective medium theory of Bruggeman[53] and Landauer.[54] This formalism allows calculation of an effective long-range diffusion coefficient in the presence of diffusion obstacles.[55] We consider a phase, occupying an area fraction x, with a diffusion coefficient D_m, in which domains with diffusion coefficient D_d and an area fraction $(1 - x)$ are dispersed. Of particular interest here is the case in which the domains are impermeable obstacles ($D_d = 0$), since the relative bulky BODIPY probe lipid is not likely to enter the ordered lipids[56] immediately under the bound protein. In this limit of impermeable obstacles the effective medium theory is valid for an obstacle area fraction up to 0.2. In this range, the effective diffusion coefficient through the heterogeneous medium, D_{eff}, is given by $D_{eff}(T) = (2x - 1)D_m(T)$.[55] Using the diffusion coefficients of protein-free DMOPC membranes as $D_m(T)$ at different temperatures, we perform a one-parameter fit of the above expression to the diffusion coefficients obtained from DMOPC membranes with bound CTB (Figure 4). The fit gives an area fraction of impermeable domains $(1 - x)$ of 0.07 ± 0.03, which is in agreement with the 0.09 area fraction of the membrane covered by CTB in these experiments (the details of the latter estimate are described below). Unlike DMOPC, DMPC membranes are, for the most part, composed of a mixture of gel and fluid phases throughout the investigated temperature range, regardless of the presence of protein (see IR spectroscopy results below). Hence, the effective medium theory, based on protein associated diffusion obstacles, is not capable of describing the reduction in D caused by protein binding in the case of DMPC, and other mechanisms must be considered.

3.2. Concentration Dependent Diffusion Measurements. Next, D_b/D_0 in DMPC membranes at T_m is determined as a function of bound protein concentration. We find that long range lipid diffusion through the DMPC membrane is sensitively dependent on the amount of CTB present, and as little as 5 nM CTB in solution, corresponding to an area coverage of 0.02,

(49) Benda, A.; Benes, M.; Marecek, V.; Lhotsky, A.; Hermens, W. T.; Hof, M. *Langmuir* **2003**, *19*, 4120−4126.
(50) Widengren, J.; Mets, U.; Rigler, R. *J. Phys. Chem.* **1995**, *99*, 13368−13379.
(51) Chen, Y.; Muller, J. D.; Eid, J. S.; Gratton, E. In *New Trends in Fluorescence Spectroscopy: Applications to Chemical and Life Sciences*; Valeur, B., Brochon, J. C., Eds.; Springer: Berlin, 2001; pp 277−302.
(52) Cevc, G. *Biochemistry* **1991**, *30*, 7186−7193.
(53) Bruggeman, D. A. G. *Ann. Phys. (Leipzig)* **1935**, *24*, 636−664.
(54) Landauer, R. *J. Appl. Phys.* **1952**, *23*, 779−784.
(55) Saxton, M. J. *Biophys. J.* **1982**, *39*, 165−173.
(56) Burns, A. R.; Frankel, D. J.; Buranda, T. *Biophys. J.* **2005**, *89*, 1081−1093.

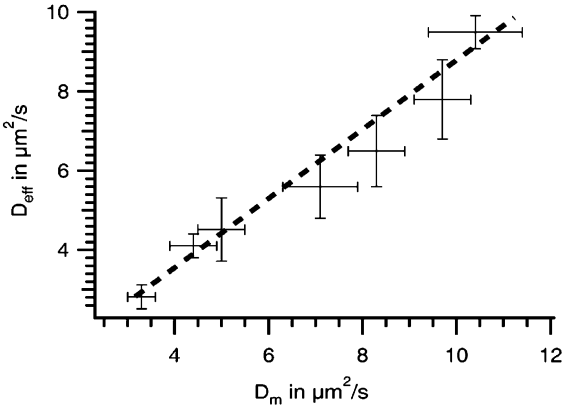

Figure 4. Diffusion coefficients of DMOPC membranes with CTB induced obstacles (D_{eff}) as a function of the protein-free diffusion coefficient (D_m). The dashed line represents the one-parameter fit to the effective medium theory by Bruggeman and Landauer, yielding an obstacle area fraction of 0.07 ± 0.03.

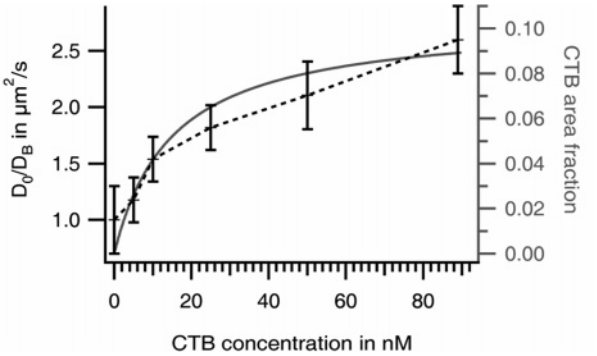

Figure 5. Diffusion coefficient ratio D_b/D_0 for the DMPC membrane at 23.3 °C (black) depends on the solution concentration of CTB and exhibits a monotonic increase with the area fraction occupied by CTB (gray).

already leads to a 15% reduction in probe mobility (Figure 5, black line). The area fraction of the membrane surface covered by bound CTB is computed in the following way: One CTB binds, on average, 2 GM_1 molecules.[57] The binding equilibrium of the two-step process, which involves initial docking of CTB to one GM_1 and subsequent scavenging of a second GM_1, can be described by an effective binding constant K_d. Hence, the concentration of free CTB in solution ($[CTB_f]$), the initial GM_1 concentration ($[GM_1]$) of 1.4×10^{-11} nM/μm^2, and K_d (= 30 nM, from[58]) are related to the concentration of surface bound CTB ($[CTB_b]$) via $[CTB_b] = [CTB_f]([GM_1{}^0] - 2[CTB_b])/K_d$. Solving for $[CTB_b]$ and assuming an area cross-section of CTB of 25 nm^2 [59] and equipartition of GM_1 between both membrane leaflets yields the area fraction plotted in Figure 5 (gray line).

3.3. Temperature-Dependent IR Spectroscopy Measurements. To investigate the connection between long-range diffusion behavior and conformational changes of the membrane lipids and associated lipid phases, AIR-FTIR spectra on GM_1/DMPC single membranes[46] were measured as a function of temperature, before and after CTB-binding (Figure 6B and 6C). The two sets of absorption bands can be straightforwardly assigned to the methylene symmetric and asymmetric stretching modes.[39] Their details including the exact location of peaks,

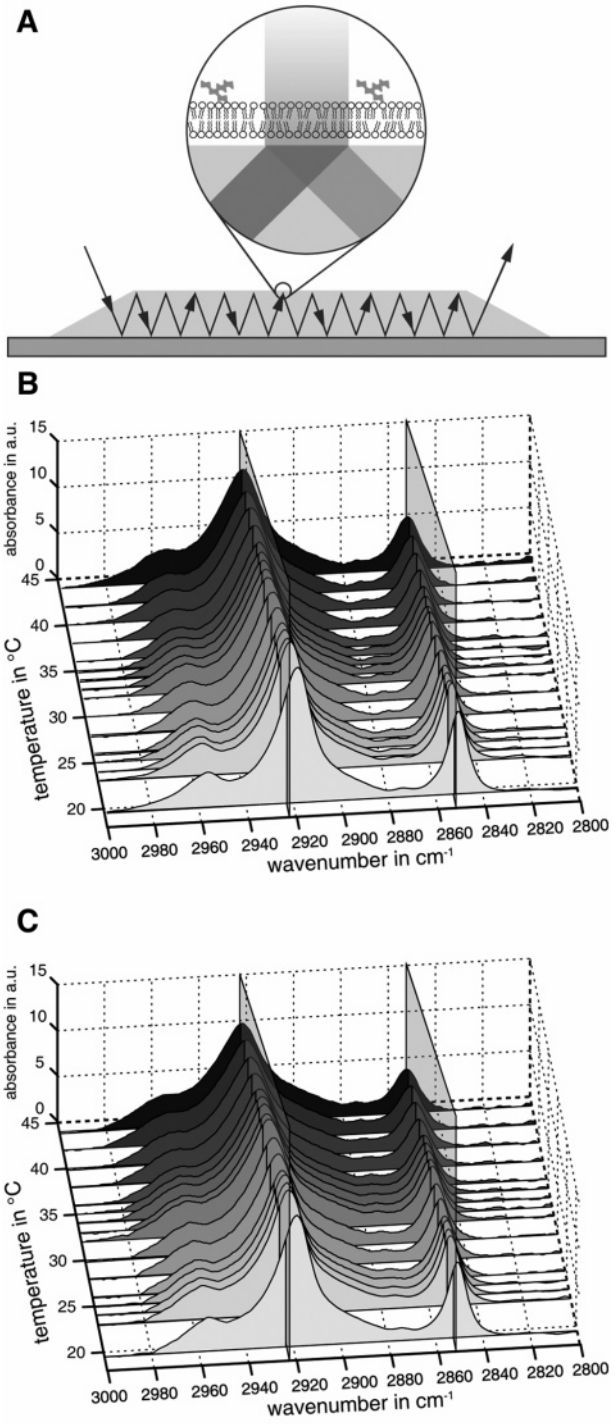

Figure 6. (A) Schematic of AIR-FTIR spectroscopy, showing the Si internal reflection element (IRE) and the IR beam undergoing total internal reflection. A single membrane is deposited on one side of the IRE, allowing for IR absorption of the lipids in the evanescent field (blow up). (B) AIR-FTIR spectra of a GM_1 doped DMPC membrane in the temperature range 19.5−44 °C in the absence of CTB (B) and with CTB bound to the membrane (C).

their full-width half-maxima, and relative intensity distributions are in good agreement with the earlier reports of infrared spectra of DMPC membranes.[60] The exact locations of the methylene symmetric and asymmetric stretching, d+ and d−, modes are well-known diagnostic markers in the determination of chain-

(57) Lauer, S.; Goldstein, B.; Nolan, R. L.; Nolan, J. P. *Biochemistry* **2002**, *41*, 1742−1751.
(58) Winter, E. M.; Groves, J. T. *Anal. Chem.* **2006**, *78*, 174−180.
(59) Wang, R.; Shi, J.; Parikh, A. N.; Shreve, A. P.; Chen, L. H.; Swanson, B. I. *Colloids Surf., B* **2004**, *33*, 45−51.
(60) Tamm, L. K.; Tatulian, S. A. *Q. Rev. Biophys.* **1997**, *30*, 365−429.

conformational order. In solid crystalline phases, the symmetric methylene stretching (d+) of alkyl chains absorbs between 2848 and 2850 cm^{-1}, and the asymmetric stretching (d−) occurs between 2916 and 2918 cm^{-1}. For a conformationally disordered liquid phase, however, absorptions due to d+ and d− modes occur at distinctly higher ranges of 2856−2858 cm^{-1} and 2924−2928 cm^{-1}, respectively.[61] The two sets of bands, d+ and d−, gradually shift toward higher frequencies as the temperature is raised from 19.5 °C to 44 °C for both the unbound and bound states, suggesting that the membrane assembly was predominantly in the L_β gel phase below the transition temperature (23 °C) and gradually transformed into the fluid L_α state as the temperature increased (Figure 6). The transition spans, in both cases, an extended temperature range of more than 15 °C, which is in accord with recent studies on supported lipid membranes.[62−64] SLBs have, in general, a much broader main transition than free lipid membranes. Although the positions of the IR absorption peaks follow a similar trend with increasing temperature, the degree of chain order in the protein bound state is observed to be different from that in the unbound state in the range 25−42 °C as reflected by the difference in the peak locations (Figure 7A and 7B). The d+ and d− frequencies observed within this temperature range revealed relatively higher chain ordering in the bound state, indicating that the CTB−GM_1 binding event triggered changes in the lipid phase state and chain organization. In addition, from the spectral changes the area fraction of the gel phase for membranes with and without bound CTB (Figure 7C) can be estimated as described in the Materials and Methods section. The maximal difference is on the order of 0.2, which, interestingly, is significantly larger than the 0.09 area fraction of membrane covered directly by CTB under these conditions. This suggests that the protein induced order extends beyond the immediate binding site. At temperatures higher than 38 °C, the difference in gel phase area fractions vanishes. Thus, lipids in the vicinity of bound protein will eventually undergo the conformational transition, but at higher temperatures.

It is interesting to note that whereas the FCS data indicate the largest impact of protein binding on lipid diffusion at T_m, no measurable increase in gel phase is observed by FTIR. This excludes large changes in the gel and fluid lipid fractions as the leading cause of the diffusion retardation at T_m in the presence of the protein. Since the maximal area fraction of protein is less than 0.1 in our experiments (Figure 5), the retardation of the mobility due to viscous coupling of the membrane to a continuous layer of proteins in proximity[65] can be immediately ruled out. A mechanism in which lipids diffuse together as patches that are organized by larger molecules adsorbed at the membrane surface[35] is also unlikely. Zangh et al. find that in such cases of slaved diffusion the molecule needs to cover at least 80 lipid headgroups to cause a measurable effect. The DMPC cross-section area is about 0.6 nm^2;[66] one CTB with an area of 25 nm^2 covers approximately 35 lipids. While CTB aggregation into larger clusters cannot be completely ruled out,[59] the effect of slaved diffusion should lead to a comparable reduction throughout the entire temperature range and for both DMPC and DMOPC membranes, contrary to observation. Furthermore, in the case of "slaved" diffusion, both the slow diffusive process due to collective lipid motion and the fast diffusion of free lipids are detected. Our correlation data, however, are well described with a one-component diffusion model. In addition, the DMOPC data suggest that the CTB associated membrane is mostly impermeable to the lipid probe.

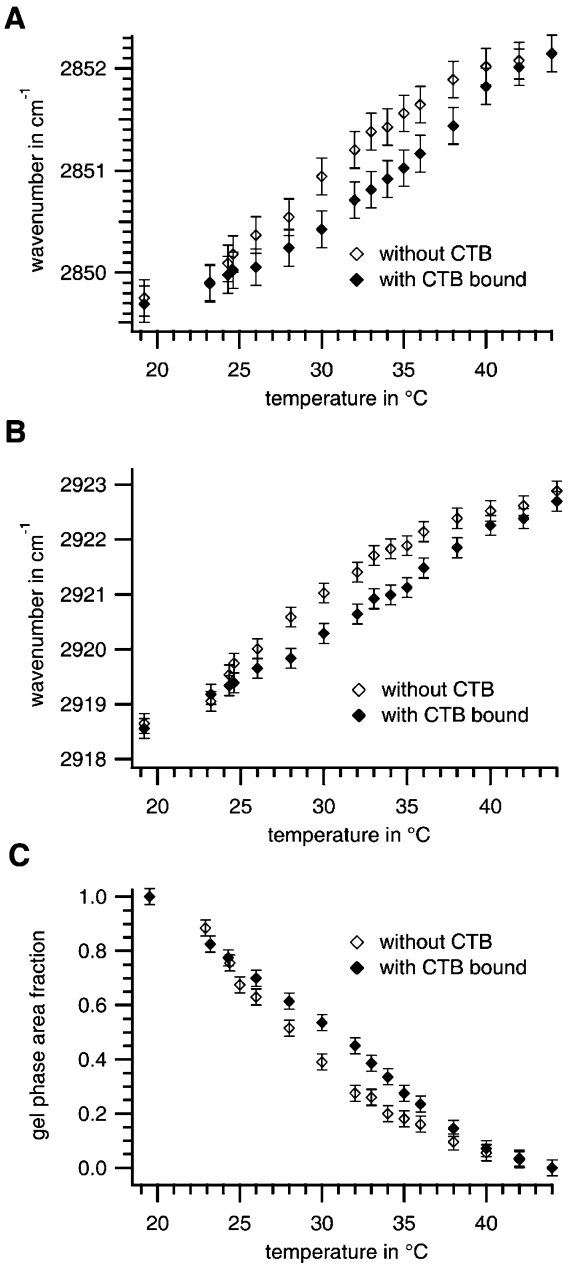

Figure 7. Positions of the absorption peaks of symmetric (A) and asymmetric (B) methylene stretching vibrations with respect to temperature for both the unbound (◇) and the bound states (◆). (C) Average gel phase area fraction as a function of temperature in the presence (◆) and absence (◇) of CTB.

4. Conclusion

All our experimental findings can be reconciled by the following picture: Below the phase transition all diffusion must occur through the gel phase. With the onset of the transition,

(61) Snyder, R. G.; Schachtschneider, J. H. *Spectrochim. Acta* **1963**, *19*, 85−116.
(62) Enders, O.; Ngezahayo, A.; Wiechmann, M.; Leisten, F.; Kolb, H. A. *Biophys. J.* **2004**, *87*, 2522−2531.
(63) Garcia-Manyes, S.; Oncins, G.; Sanz, F. *Biophys. J.* **2005**, *89*, 4261−4274.
(64) Xie, A. F.; Yamada, R.; Gewirth, A. A.; Granick, S. *Phys. Rev. Lett.* **2002**, *89*.
(65) Evans, E.; Sackmann, E. *J. Fluid Mech.* **1988**, *194*, 553−561.
(66) Marra, J.; Israelachvili, J. N. *Biochemistry* **1985**, *24*, 4608−4618.

channels of fluid lipid phase form[62−64] and probe lipids will preferentially partition into these leads.[56] As long as the melting lines do not interconnect, the observed averaged long-range mobility will be dominated by the gel phase diffusion coefficients. Once the fluid channels percolate, however, the majority of the transport observed by FCS will be governed by the faster diffusion in the fluid phase. As the IR data indicate, binding of CTB to GM_1 organizes the lipids in the membrane beneath the binding site. Since GM_1 partitions into the gel phase,[56] this additional order will be buried in the large gel phase fraction present at the onset of the transition. Thus, it will not be visible in the IR spectra in the proximity of T_m. However, these strongly ordered domains should have a significant impact on long-range diffusion by suppressing the formation and interconnection of the L_α phase channels at the initial stages of the main transition. Only a small change, not resolvable by AIR-FTIRS, in the amount and organization of the L_α phase would be necessary to prevent sufficient percolation of the melting lines. Hence, in the proximity of the transition, long-range mobility in the presence of protein will still be dominated by diffusion through the gel phase, whereas, in the absence of protein, it is already largely governed by diffusive transport in interconnected fluid phase channels. Such a mechanism will sensitively depend on the amount of membrane-bound protein, which is indeed seen in the concentration dependent FCS measurements. At higher temperatures, the protein associated membrane patches serve as diffusion obstacles and account for the slight reduction in D.

Acknowledgment. M.B.F. wants to thank Esther Winter, Nathan Clack, and Andrew DeMond for helpful discussions. This work has been supported by funding from the National Science Foundation. The Center for Biophotonics, an NSF Science and Technology Center is managed by the University of California, Davis, under Cooperative Agreement No. PHY 0120999.

Supporting Information Available: Detailed descriptions of the materials, the methods, the techniques, and the data analysis of the experiments. This material is available free of charge via the Internet at http://pubs.acs.org.

JA064093H